



Experiment Report Form

The double page inside this form is to be filled in by all users or groups of users who have had access to beam time for measurements at the ESRF.

Once completed, the report should be submitted electronically to the User Office via the User Portal:
<https://www.esrf.fr/misapps/SMISWebClient/protected/welcome.do>

Deadlines for submission of Experimental Reports

Experimental reports must be submitted within the period of 3 months after the end of the experiment.

Experiment Report supporting a new proposal (“relevant report”)

If you are submitting a proposal for a new project, or to continue a project for which you have previously been allocated beam time, you must submit a report on each of your previous measurement(s):

- even on those carried out close to the proposal submission deadline (it can be a “*preliminary report*”),
- even for experiments whose scientific area is different from the scientific area of the new proposal,
- carried out on CRG beamlines.

You must then register the report(s) as “relevant report(s)” in the new application form for beam time.

Deadlines for submitting a report supporting a new proposal

- 1st March Proposal Round - **5th March**
- 10th September Proposal Round - **13th September**

The Review Committees reserve the right to reject new proposals from groups who have not reported on the use of beam time allocated previously.

Reports on experiments relating to long term projects

Proposers awarded beam time for a long term project are required to submit an interim report at the end of each year, irrespective of the number of shifts of beam time they have used.

Published papers

All users must give proper credit to ESRF staff members and proper mention to ESRF facilities which were essential for the results described in any ensuing publication. Further, they are obliged to send to the Joint ESRF/ ILL library the complete reference and the abstract of all papers appearing in print, and resulting from the use of the ESRF.

Should you wish to make more general comments on the experiment, please note them on the User Evaluation Form, and send both the Report and the Evaluation Form to the User Office.

Instructions for preparing your Report

- fill in a separate form for each project or series of measurements.
- type your report in English.
- include the experiment number to which the report refers.
- make sure that the text, tables and figures fit into the space available.
- if your work is published or is in press, you may prefer to paste in the abstract, and add full reference details. If the abstract is in a language other than English, please include an English translation.



	Experiment title: 3D strain analysis across a shear band by tomographic reconstruction	Experiment number: HC-3829
Beamline: ID11	Date of experiment: from: 01.11.2018 to: 06.11.2018	Date of report:
Shifts: 12	Local contact(s): Jonathan Wright	<i>Received at ESRF:</i>
Names and affiliations of applicants (* indicates experimentalists): Sergio Scudino*, IFW Dresden Helmholtzstrasse 20, 01069 Dresden, Germany Junhee Han*, IFW Dresden Helmholtzstrasse 20, 01069 Dresden, Germany		

Report:

Despite the experimental difficulties posed by the nanoscale size of shear bands, a significant advance in understanding the mechanism of shear band formation in metallic glasses has been attained recently using a variety of techniques, including TEM, nanoindentation, XRD and magnetic measurements. In these techniques, shear bands are considered as linear defects propagating in a 2D sample and, therefore, it is implicit that the observed 2D properties are characteristic also of the missing direction. A typical example is XRD strain analysis, where the output is a strain averaged over the thickness of the specimen. Shear bands are, however, planar defects and the strain may change across the thickness.

Tomographic techniques using X-rays represent the ideal tool for extending the XRD investigations of shear bands in metallic glasses to the missing direction. X-ray absorption (or phase contrast) computed tomography (XCT or PCT) have been recently employed to analyze void and crack formation in metallic glasses. However, XCT or PCT are not able to detect shear bands yet because density variations and thickness of a shear band are at the moment below the detection limit. Therefore, in our experiment we turned to X-ray diffraction tomography (XRDCT).

The 2D diffraction pattern from a metallic glass is in principle circular; however, a detectable elliptical distortion (especially visible in the position of the first sharp diffraction peak) is introduced when there is sufficient elastic strain in the specimen. Our recent 2D XRD experiments have shown that shear band formation generates a characteristic antisymmetric strain field in the adjacent material (Fig. 1). In our experiment, we utilized this distinctive strain profile to identify the shear band paths within a plastically-deformed metallic glass via XRDCT.

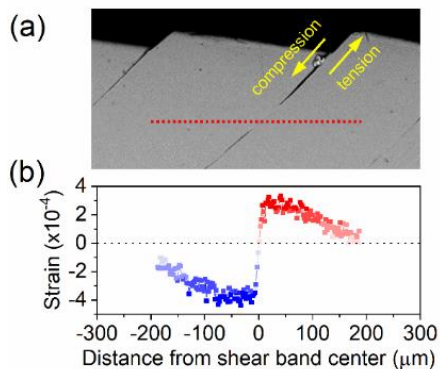


Fig. 1. (a) Characteristic shear band morphology of a plastically-deformed metallic glass and (b) strain profile across a shear band (corresponding to the red dots in (a)) derived by 2D XRD.

We designed the XRD setup to have the tomographic axis parallel to the shear band direction (red plane in Fig. 2). This ensures that the strain component along the tomographic axis (ϵ_{zz}) can be reconstructed meaningfully. 2D diffraction patterns ($\lambda = 0.20664 \text{ \AA}$; beam size $1 \times 1 \mu\text{m}^2$) were recorded every $1 \mu\text{m}$ along a line perpendicular to the shear band direction while the specimen was rotating around the tomographic axis. For each point on the line, starting from the rotation axis, 180 projections with angular step $\omega = 2^\circ$ were acquired to cover a 360 degree range. Long term positioning drifts were compensated by periodically repositioning the specimen using a signal from some sharp diffraction peaks due to crystalline surface impurities. The data were corrected for the geometrical

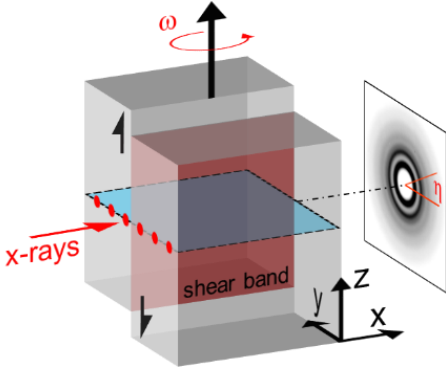


Fig. 2. Schematic of the XRDCT setup. The red plane parallel to the z axis (i.e. the tomographic axis) represents the shear band and the blue plane is the slice investigated by strain tomography.

effect of the sample shape by assuming a simple rectangular shape and computing an average sample to detector distance for each frame as a function of y position and angular step ω .

Because of the extremely large number of 2D images necessary for the reconstruction, data processing was carried out on-site during the experiment using python scripts. The 2D patterns were integrated in 5° azimuthal slices between 0 and 360° using the pyFAI program to give intensity distributions $I(q)$ as a function of the scattering vector q for each combination of y , ω and azimuthal angle η . We focused the analysis on the first scattering maximum (q_1) in reciprocal space to optimize the diffraction experiment and reduce systematic errors in the following tomographic strain reconstruction. The values of $\sqrt{q_1}$ for each y , ω and η were determined by fitting the integrated patterns using a pseudo-Voigt. The square root scale gives a symmetric peak shape for this sample, which improves the fitting procedure.

A Fourier series as a function η was then employed to fit the peak position q_1 as:

$$\sqrt{q_1(\eta)} = c_0 + (c_1 \sin \eta + c_2 \cos \eta) + (c_3 \sin 2\eta + c_4 \cos 2\eta)$$

in order to distinguish the individual contributions to the elliptical distortion of $q_1(\eta)$ due to beam center shift ($\sin \eta$ terms) and strain ($\sin 2\eta$ terms). Outlier data with more than 5X median absolute deviations of observed from calculated were considered as corrupted by crystalline peaks and excluded from the reconstruction. The strain component along the tomographic axis (ε_{zz}) for each y position and sample rotation ω were then obtained via:

$$q_0 = (\text{median}(c_0))^2, \quad q_z = (c_0 - c_4)^2$$

$$\varepsilon_{zz} = \frac{(q_0 - q_z)}{q_z}$$

In our calculation, we assume the scattering angle to be small enough that the strain along the z direction is equivalent to the strain along the scattering vector. This assumption may introduce an error of about 5 % ($= \sin \theta$) for contamination of ε_{zz} by the components away from the tomographic axis. The tomographic reconstruction was performed according to Korsunsky et al. [*Acta Mater.* 59 (2011) 2501]. The shape of the specimen was first reconstructed from the fitted peak heights via filtered back projection. A threshold was applied to this image and, assuming uniform scattering density, a mask image was produced and back transformed to produce a sinogram (radon function) of the sample thickness (T). This method was used to reduce artifacts introduced by intensity

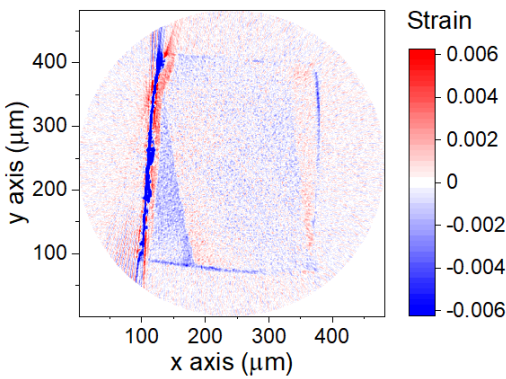


Fig. 3. Shear band paths reconstructed via XRD strain tomography using the strain parallel to the tomographic axis (ε_{zz}).

fluctuations, or noisy data due to crystalline impurities. The strain sinogram was then generated multiplying the sinogram of measured peak shifts due to strain by the sample thickness. In the case of a strain component parallel to the z -axis (tomographic axis), the inversion of the strain sinogram (via iradon) approximately gives the image of the strain component along z , where the paths of two shear bands within the specimen are clearly observable (Fig. 3).

This experiment demonstrates that the path of shear bands can be reconstructed via XRDCT using the strain fields generated by shear bands. Therefore, we consider this measurement to have been a large success and we have, to a great degree, accomplished our goals outlined in the proposal. No experimental difficulties were encountered and the scientific support from the local contact was simply outstanding.